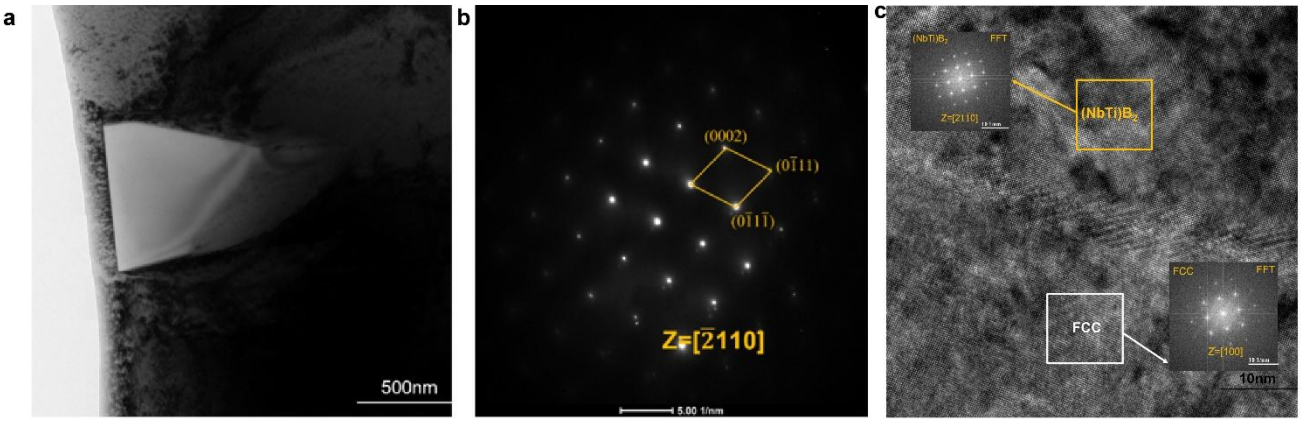
Supplementary Table 1

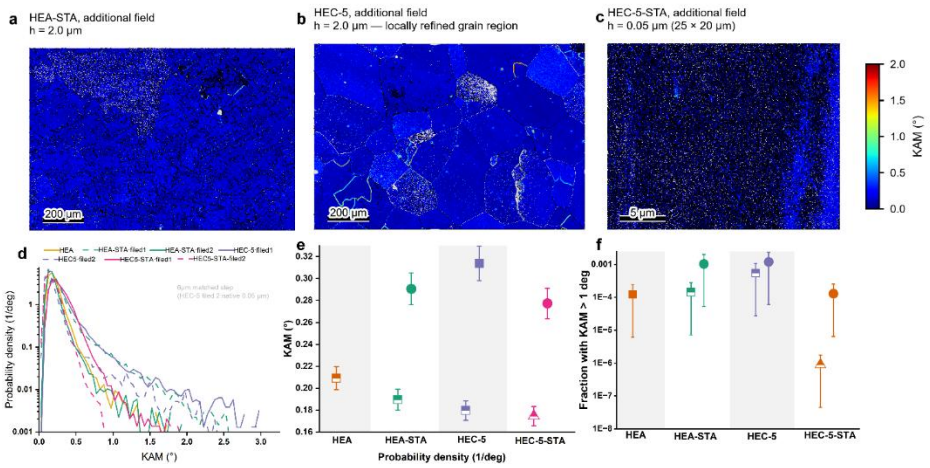
Condition	Grains analysed, *n*	Mean (μm)	s.d. (μm)	Median (μm)	Range (μm)	Area-weighted mean (μm)	>100 μm, *n*	<10 μm, *n*
HEA	523	18.03	42.26	9.30	6.38–459.72	287.98	13	303
HEA-STA	629	16.67	35.24	8.74	6.38–504.72	268.75	13	395
HEC-5	14	263.06	189.92	210.06	23.70–583.67	449.68	10	0
HEC-5-STA	9	315.25	239.27	341.17	12.57–743.81	554.30	6	0

Supplementary Table 1 Grain-size statistics of the four alloy conditions. Grain-size statistics obtained from EBSD datasets for HEA, HEA-STA, HEC-5 and HEC-5-STA. The table reports the number of individual grains analysed (*n*), arithmetic mean, standard deviation (s.d.), median, grain-size range, area-weighted mean grain size, and the numbers of grains larger than 100 μm and smaller than 10 μm. Here, *n* denotes the number of individual grains included in the analysis rather than the number of independently prepared specimens.



Supplementary Fig. 1

Additional crystallographic characterization of an AlB_2-type Nb/Ti-containing boride in HEC-5. a, Representative TEM image of the analysed boride particle in the as-cast HEC-5 alloy. b, Corresponding selected-area electron diffraction (SAED) pattern indexed to the hexagonal AlB_2-type $(Nb,Ti)B_2$ structure, with indexed reflections shown for the $[2\,\bar{1}\bar{1}\,0]$ zone axis. c, HRTEM image of a representative $(Nb,Ti)B_2$/FCC interfacial region. The boxed regions are enlarged in the insets to show lattice fringes from the boride and neighbouring FCC matrix, respectively.



Supplementary Fig. 2 Additional EBSD fields and field-resolved KAM/GND statistics. a–c, KAM maps of three EBSD fields that are not used in Fig. 2 or Fig. 4. a, an additional HEA-STA field (step h = 2.0 µm; 1302 × 894 µm). b, an additional HEC-5 field (h = 2.0 µm) sampling a locally refined grain region. c, an additional HEC-5-STA field acquired at h = 0.05 µm over 25 × 20 µm, resolving fine-scale orientation gradients; this microfield is not used to infer bulk grain size. Black lines mark boundaries with misorientation ≥10°; grey denotes unindexed pixels; colour scale, 0–2°. d, KAM probability densities: six fields resampled to a common 6 µm grid; the 0.05 µm field is shown at its native step (dotted) because a 6 µm grid retains only 9 points there, so that curve is not comparable with the others. e,f, field-level summaries of field-mean KAM (e) and of the fraction of points with KAM > 1° (f); symbols denote individual fields (filled, field of Fig. 2 or Fig. 4; open square, additional field; open triangle, additional field at the native 0.05 µm step) and vertical bars span the 5th–95th percentile of non-overlapping 180 µm sub-windows within each field (5 µm for c); where the 5th percentile is zero, the lower end of the bar is drawn at the plotting floor. Maps are drawn at true pixel aspect. KAM is recomputed from raw orientation data with a first-order eight-neighbour kernel, a 5° cutoff and ≥3 valid neighbours; the GND-density proxy is $\rho = 2\theta/(hb)$, with b = 0.2528 nm. Because ρ depends on h, between-condition comparisons among macroscale fields use the common 6 µm grid.

Supplementary Table 2 EBSD and KAM/GND analysis summary

Condition / field	Native step size (μm)	Map size (μm × μm)	Analysis step, h (μm)	Valid FCC KAM points, n	Mean KAM (°)	KAM > 1° (%)	Mean GND density (m^{-2})	Median GND density (m^{-2})	GND density, 5th–95th percentile (m^{-2})
HEA	2	1302 × 894	6	28,393	0.216	0.6	4.97×10^{12}	4.31×10^{12}	2.33×10^{12} – 9.26×10^{12}
HEA-STA-1	2	1302 × 894	6	27,851	0.293	2.11	6.73×10^{12}	5.30×10^{12}	2.77×10^{12} – 1.61×10^{13}
HEA-STA-2	2	1302 × 894	6	27,699	0.189	0.28	4.36×10^{12}	3.82×10^{12}	2.16×10^{12} – 8.01×10^{12}
HEC-5-1	3	1302 × 894	6	32,206	0.317	2.48	7.29×10^{12}	5.68×10^{12}	2.85×10^{12} – 1.67×10^{13}
HEC-5-2	2	1302 × 894	6	31,138	0.187	1.46	4.30×10^{12}	3.19×10^{12}	1.66×10^{12} – 9.24×10^{12}
HEC-5-STA-1	2	1282 × 864	6	30,012	0.277	0.27	6.38×10^{12}	5.69×10^{12}	2.83×10^{12} – 1.19×10^{13}
HEC-5-STA-2†	0.05	25 × 20	0.05	162,169	0.174	0.0019	4.82×10^{14}	4.35×10^{14}	1.95×10^{14} – 9.15×10^{14}

HEC-5-STA-2 is a 25 × 20 μm microfield measured at h = 0.05 μm. Its KAM/GND statistics are native-step descriptors and should not be directly compared with the six 6 μm-grid macroscale fields.

Supplementary Note 1. Microstructural sampling

The EBSD archive contains seven named fields: one HEA field and two fields each for HEA-STA, HEC-5 and HEC-5-STA (Supplementary Table 2). Six macroscale fields were analysed on a common 6 μm grid. The second HEC-5-STA field covers 25 × 20 μm at a 0.05 μm native step and is retained for local orientation-gradient description. The $L1_2$ diameter and spacing measurements in Fig. 3j,k were taken from two TEM fields (126 precipitates and 63 spacings). Field identifiers and measured grains or pixels do not establish independently melted ingot replication; ingot identifiers for microscopy were absent from the supplied EBSD and TEM archives.

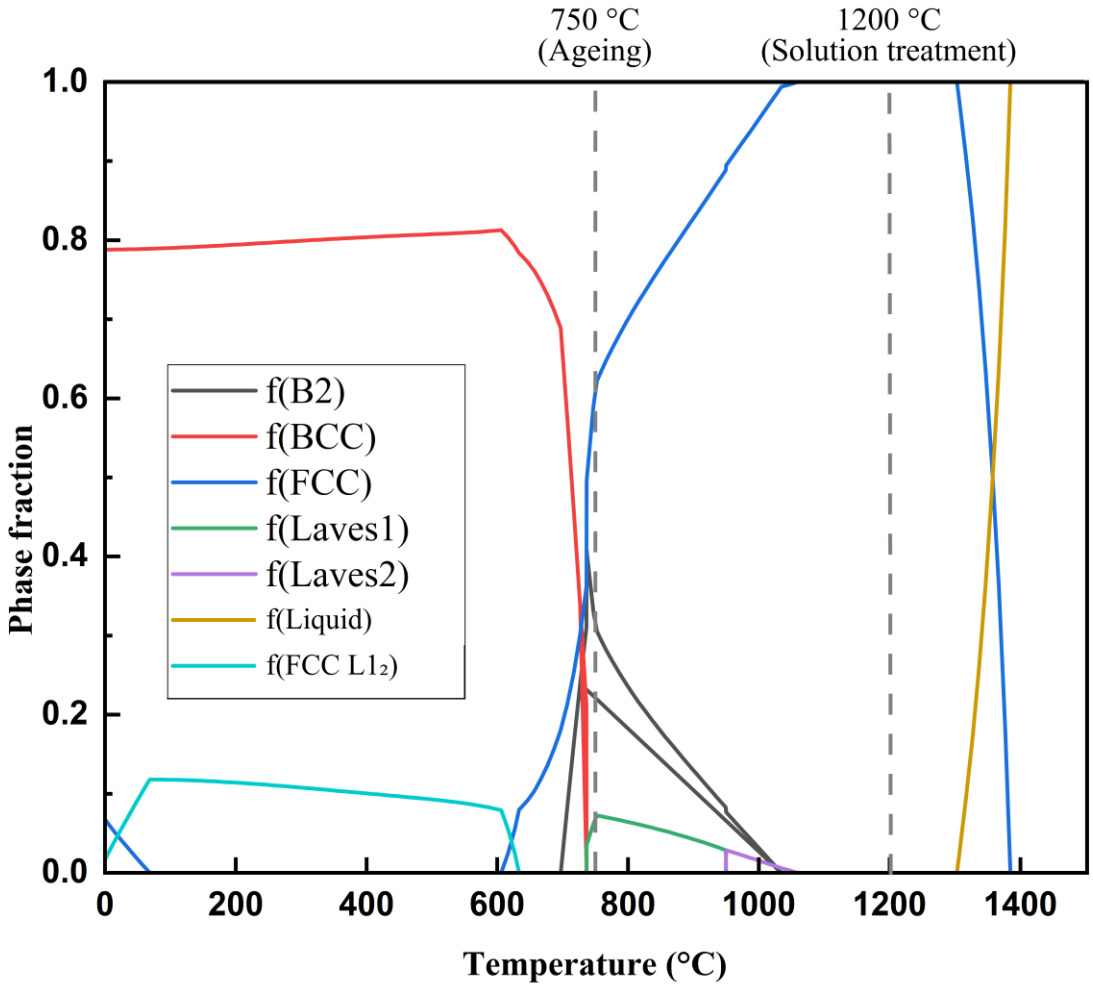
Supplementary Note 2. CALPHAD calculation scope and assumptions

Equilibrium CALPHAD calculations were performed for the nominal $Fe_{35}Co_{30}Ni_{25}Al_7Nb_3$ (at.%) base-alloy

composition using Thermo-Calc 2025 with the TCHEA8 database. The calculation did not include Ti or B introduced through the Al–TiB_2 master alloy or reaction-generated local chemical heterogeneity. It was used only to guide selection of the 1,200 °C solution-treatment and 750 °C ageing temperatures and should not be interpreted as a prediction of the precipitation sequence, phase morphology or local chemistry in HEC-5.

Supplementary Table 3 CALPHAD calculation settings and assumptions

Parameter	**Setting or assumption**
Software	Thermo-Calc 2025
Thermodynamic database	TCHEA8
Nominal alloy composition	$Fe_{35}Co_{30}Ni_{25}Al_7Nb_3$ (at.%)
Calculation type	Equilibrium CALPHAD calculation
Calculated quantity	Equilibrium phase fractions as a function of temperature
Compositional basis	Nominal base-alloy composition
Solution-treatment temperature	1,200 °C
Ageing temperature	750 °C
Treatment of Ti/B and reaction-generated local chemical heterogeneity	Not included; the calculation used the nominal Ti/B-free base-alloy composition
Interpretation	Thermodynamic guidance only; not a prediction of precipitation sequence, phase morphology or reaction-generated local chemistry



Supplementary Fig. 3 Calculated equilibrium phase fractions for the nominal base alloy. Equilibrium phase fractions as a function of temperature for $Fe_{35}Co_{30}Ni_{25}Al_7Nb_3$ (at.%), calculated using Thermo-Calc 2025 with the TCHEA8 database. Dashed lines mark the 750 °C ageing and 1,200 °C solution-treatment temperatures. The calculation uses the nominal base-alloy composition and excludes Ti/B additions and reaction-generated local chemical heterogeneity; it is presented as thermodynamic guidance rather than as a prediction of the precipitation sequence, phase morphology or local chemistry in HEC-5.